The Journal of Chemical Physics

Examining solvent effects on the ultrafast dynamics of catechol

Cite as: J. Chem. Phys. **151**, 084305 (2019); https://doi.org/10.1063/1.5116312@jcp.2019.FEMTO2019.issue-1
Submitted: 24 June 2019 . Accepted: 01 August 2019 . Published Online: 27 August 2019

M. A. P. Turner, R. J. Turner, M. D. Horbury, N. D. M. Hine, and V. G. Stavros

The Journal of Chemical Physics ARTICLE scitation.org/journal/jcp

Examining solvent effects on the ultrafast dynamics of catechol

Cite as: J. Chem. Phys. 151, 084305 (2019); doi: 10.1063/1.5116312
Submitted: 24 June 2019 • Accepted: 1 August 2019 •
Published Online: 27 August 2019

M. A. P. Turner,[1,2] R. J. Turner,[2] M. D. Horbury,[2] N. D. M. Hine,[1] and V. G. Stavros[2,a)]

AFFILIATIONS

[1] Department of Physics, University of Warwick, Coventry, CV47AL, United Kingdom
[2] Department of Chemistry, University of Warwick, Coventry, CV47AL, United Kingdom

Note: The paper is part of the JCP Special Topic on Ultrafast Molecular Sciences by Femtosecond Photons and Electrons.
[a)] v.stavros@warwick.ac.uk

ABSTRACT

We consider the effect of a polar, hydrogen bond accepting, solvent environment on the excited state decay of catechol following excitation to its first excited singlet state (S_1). A comparison of Fourier transform infrared spectroscopy and explicit-solvent *ab initio* frequency prediction suggests that 5 mM catechol in acetonitrile is both nonaggregated and in its "*closed*" conformation, contrary to what has been previously proposed. Using ultrafast transient absorption spectroscopy, we then demonstrate the effects of aggregation on the photoexcited S_1 lifetime: at 5 mM catechol (nonaggregated) in acetonitrile, the S_1 lifetime is 713 ps. In contrast at 75 mM catechol in acetonitrile, the S_1 lifetime increases to 1700 ps. We attribute this difference to aggregation effects on the excited-state landscape. This work has shown that explicit-solvent methodology is key when calculating the vibrational frequencies of molecules in a strongly interacting solvent. Combining this with highly complementary steady-state and transient absorption spectroscopy enables us to gain key dynamical insights into how a prominent eumelanin building block behaves when in polar, hydrogen bond accepting solvents both as a monomer and as an aggregated species.

I. INTRODUCTION

The Sun can be approximated as a classical black-body radiator, emitting a broad range of light centered in the visible region of the electromagnetic spectrum (400–800 nm). Although the bulk of the radiation reaching the Earth's surface is within this visible region, approximately 6% is in the form of ultraviolet (UV) radiation.[1]

Without photoprotection from UV radiation, many biomolecules essential for life, such as nucleobases in DNA, would be quickly degraded, leading to extensive mutagenesis and other unwanted effects.[2] Melanin is a class of pigment found in humans, providing a pertinent example of how nature seeks to mitigate these effects, with eumelanin being the most prominent.[3–6] Although the exact structure of eumelanin is not entirely clear, it is known to be a heterogeneous macromolecule comprising multiple subunits including dihydroxyindole (DHI) and dihydroxyindole-2-carboxylic acid (DHICA), shown in Fig. 1.[7–10] Eumelanin has many other functions attributed to it aside from photoprotection. Some of these include thermal-regulation, cation chelation, antibiotic properties, and acting as a free-radical sink.[2,11–13] Intermolecular hydrogen bonding has previously been shown to be an important factor in the photoprotection of eumelanin, both through stabilization of photoproducts and through direct interaction.[14,15]

It had previously been shown that catechol has a key role in the photoprotection provided by eumelanin.[16] To study the photoprotective properties of eumelanin, a bottom-up approach was employed by Horbury *et al.*, using 4-*tert*-butylcatechol (4-TBC), an analog of catechol with greater solubility in cyclohexane (a property that was useful for this work).[17] Transient Electronic (UV/visible) Absorption Spectroscopy (TEAS) was used in conjunction with time-resolved velocity ion map imaging to determine the lifetime of excited states of 4-TBC after excitation with UV radiation at 267 nm, in both the gas- and condensed-phase. Horbury *et al.* found that the first excited singlet state (S_1, $^1\pi\pi^*$) decayed via multiple pathways, depending on which solvent 4-TBC was present in, inferred through two features in the transient absorption spectrum (TAS). First, it appears that the 4-*tert*-butylcatechoxyl radical (4-TBC$^\cdot$) is forming. This is evidenced by an absorption feature at 390 nm, notably similar

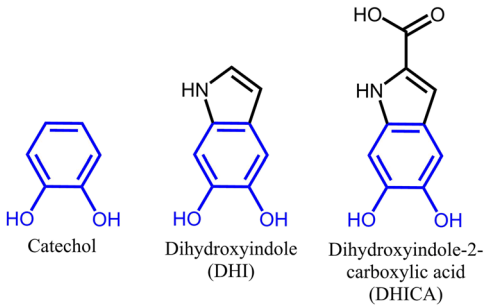

FIG. 1. Shown is (left) catechol, (center) dihydroxyindole (DHI), and (right) dihydroxyindole-2-carboxylic acid (DHICA). Catechol is a key component of different building blocks of eumelanin found in the human body. Blue highlighted catechol units show how it constitutes a key component of DHI and DHICA, important subunits of eumelanin.

to where the catechoxyl radical was observed in liquid paraffin previously (382 nm).[18,19] Second, intersystem crossing is taking place, evidenced through the broad TAS which sees a maximum at less than 350 nm and sloped across the entire probe window, a signifier of a triplet state.[20]

The lifetime of 4-TBC photoexcited to S_1 was observed to be significantly longer when dissolved in the polar solvent acetonitrile compared to when dissolved in nonpolar cyclohexane and measurements in the gas-phase. In acetonitrile, it was suggested that internal conversion (IC), fluorescence, and intersystem crossing were occurring, owing to evidence of similar processes happening in analogous systems, namely, phenol and guaiacol.[19,21,22] A kinetic isotope study involving the deuterated form of 4-TBC (4-TBC-d_2) found a fourfold increase in the lifetime of S_1 in cyclohexane. This suggests that the homolytic cleavage of the O–H bond is a barriered process.[23] The increase in the excited state lifetime in a polar solvent and the observation of a kinetic isotope effect led Horbury *et al.* to plausibly suggest that there are conformational differences in the OH groups within different solvent environments. These were defined as either *closed* or *open* conformation, and shown in Fig. 2, with the nonpolar solvent, cyclohexane, favoring the *closed* conformation. In contrast, in the polar solvent acetonitrile, 4-TBC favors the

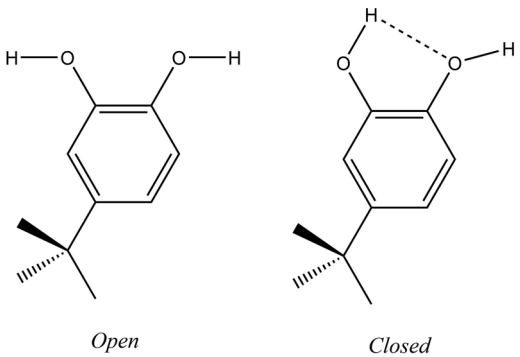

FIG. 2. *Open* and *closed* conformers of 4-*tert*-butylcatechol (4-TBC).

open conformation with two intermolecular hydrogen bonds to the solvent.

This assertion has previously been evidenced by Navarrete *et al.* who showed, through Raman spectroscopy, that catechol adopts the *open* conformer in water, acetone, and ethanol and the *closed* conformer in ether, chloroform, and benzene.[24] They went on to note that, as the previous three solvents were all highly polar and the latter three were significantly less polar, high solvent polarity leads to an *open* structure. Further to this, Varfolomeev *et al.* also proposed the breaking of the intramolecular hydrogen bond, this time in basic, hydrogen bond accepting solvents.[25] It was suggested that, ordinarily, the intramolecular hydrogen bond of catechol would have a cooperative effect on the vibrational modes of the intermolecularly bonded O–H. However, in basic, hydrogen-bond accepting solvents, this effect was no longer observed; therefore, the intramolecular hydrogen bond was likely being broken. The structure proposed by Varfolomeev *et al.* following this cleavage was not, however, an *open* structure.

Time-dependent density functional theory (TDDFT) calculations of the energy of each conformation of the S_1 state showed that while in the *open* conformation, 4-TBC remained planar, whereas the *closed* conformation buckled. Horbury *et al.* suggested that a reduction in the tunneling barrier to O–H dissociation for the buckled *closed* conformation relative to the planar *open* conformation significantly reduced the excited state lifetime.

In 2019, Grieco *et al.* built on these results, studying both the steady-state and ultrafast dynamics of varying concentrations of 4-TBC in cyclohexane.[26] In both UV-Vis and Fourier transform infrared spectroscopy (FTIR), increasing the concentration of 4-TBC in cyclohexane led to loss of fine structure and the increasing intensity of broad peaks in the steady-state spectra. This was attributed to the formation of aggregates within 75 mM 4-TBC in cyclohexane that were not present at 5 mM. This behavior is similar to that previously observed in phenol.[27–29]

The effect on the lifetime of the S_1 state of 4-TBC caused by aggregation was studied through TEAS. The results for 5 mM 4-TBC in cyclohexane were in broad agreement with that observed by Horbury *et al.* for 35 mM, with slight differences being attributed to the amount of aggregation that will have already taken place at 35 mM as opposed to 5 mM.[17] The lifetime of the S_1 state was determined to be 12 ps, predominantly decaying through the O–H dissociation pathway previously suggested. At 75 mM, however, the S_1 state decayed over a lifetime in the region of 150–200 ps. In this case, the O–H dissociation pathway having been significantly retarded was in competition with other relaxation pathways. Notably, the front-runner pathway was IC to the ground state (S_0), likely mediated through a conical intersection. Grieco *et al.* proposed that the lifetime of the O–H dissociation in this system is 190 ps and the lifetime of IC is 154 ps.[26] Owing to the similarity of these time scales, it is likely that both effects are in competition.

In the present work, we investigate the concentration dependent steady-state and time-resolved spectroscopy of catechol in acetonitrile. We use catechol (instead of 4-TBC) as no solubility issues are present in acetonitrile (which inspired the previous studies discussed *supra*), while concurrently it is a closer analog to DHI and DHICA. Furthermore, the smaller size of catechol, compared to 4-TBC, reduces the cost of computational modeling.

Our evidence strongly suggests that the primary controlling factor as to how quickly the S_1 of catechol decays is determined by the nature of the solvent environment, both through its affinity to hydrogen bond and polarity. We suggest that different hydrogen bonding environments hinder the loss of hydrogen (through O–H dissociation), both through solvent-solute interactions and through solute-solute aggregation. We also observe that polarity likely affects barrier height for both O–H dissociation and IC. Furthermore, through comparison with theoretical predictions of vibrational frequencies, we show that the monomer of catechol in acetonitrile must exist in the *closed* form, contrary to what has previously been proposed.[17,24]

II. METHODOLOGY

A. Experimental methodology

In order to carry out FTIR spectroscopy, catechol (Agros Organics, >99%) was dissolved in anhydrous acetonitrile (Sigma-Aldrich, 98%, 5 mM) under a nitrogen environment. The masking effect of water on the vibrational modes associated with the OH groups of catechol necessitated efforts to keep the solution dry. The solution was placed inside a sealed cell with pathlength 500 μm, itself located in a Bruker Vertex 70V IR spectrometer. FTIR spectroscopy was conducted with energy ranging from 500 cm^{-1} to 4000 cm^{-1} with a resolution of 1 cm^{-1}. The same methodology was followed for TEAS experiments using acetonitrile (FISCHER SCIENTIFIC, 99.8% HPLC grade); as anhydrous conditions were not essential, the nitrogen environment was also no longer necessary.

The TEAS setup was the same as used in previous studies.[22,30,31] In brief, the sample was circulated through a flow-through cell (Demountable Liquid Cell by Harrick Scientific Products, Inc.), the position of which was varied with translation stages to minimize surface aggregation. A 1 mJ/pulse 800 nm laser beam is split into two laser beams with a power ratio of 0.95:0.05. The more powerful beam was used to generate the 267 nm pump pulse through second and then third harmonic generation using two β-barium borate crystals. The remaining weaker beam was used to generate the broadband probe pulse by focusing the 800 nm incident light onto a CaF_2 window of 2 mm thickness. This window was translated vertically in order to minimize damage. The white-light probe spanned a spectral region 350–675 nm. The path lengths in the flow-through cell used for 5 mM and 75 mM solutions were, respectively, 500 μm and 56 μm. The fluence of the pump beam was ≈1–2 mJ cm^{-2}, and the absorption at both concentrations was ≈0.4 OD (where OD denotes optical density). The pump-probe time delay (Δt) was varied by altering the optical pathlength of the probe (prior to white-light generation). The instrument response function of the TEAS measurements was retrieved by fitting Gaussians to the time-zero artifacts present in pure acetonitrile and taking the full width half-maximum. These returned values of ≈80 fs; a representative data-set is shown in Fig. 1 in the supplementary material. When studying the 75 mM solution, an aggregate was observed to form on the window of the flow-through cell as the scan progressed; scans typically take 1–2 h to acquire TAS datasets (from which we obtain our transients discussed *infra*). This was evidenced by the drastically altered dynamics of the system, shortening the lifetimes extracted from our transients.

TAS in 75 mM were therefore obtained by randomly distributing all required pump-probe time-delays across six shorter scans (20 mins each), with the sample cell dismantled and cleaned whenever aggregate was observed through its excited state dynamics. The mΔOD signal from each of these data sets was normalized with pump power through matching of consecutive intensities, and the resulting TAS data were recorded as a combination of these, as depicted in Fig. 5. Confidence in this methodology is assured due to the similarity of the lifetime observed with previous literature.[17] While this was not necessary in the case of the 5 mM solution, we reduced the number of time points in order to completely remove any risk of surface aggregation. Owing to this, no data were acquired (in 5 mM samples) beyond 1.25 ns as the lifetime of this species seemed significantly shorter than this. In Fig. 5, we extrapolate these data to 2 ns for comparison with the 75 mM scan.

B. Computational methodology

We calculate predicted vibrational frequencies of catechol in the context of various implicitly and explicitly represented acetonitrile solvent environments. DFT calculations were used to optimize the proposed structures of isolated models of both the *open* and the *closed* conformers of catechol, using the NWChem package.[32] We employed the cc-pVTZ basis set and the PBE functional for initial geometry optimizations.[33,34] These calculations were performed in an implicit solvent using the COSMO solvent model for acetonitrile.[35–37] The *closed* conformer was confirmed to be the overall ground state. For the *open* form, the dihedral angles of both C–C–O–H linkages were locked in order to ensure that the *open* structure was maintained. Following this, the *open* structure was optimized without constraints to confirm that it had relaxed to a local minimum.

To map out the ground state energy surface between these minima, we then perform constrained geometry optimizations at a range of fixed dihedral angles. Results are shown in Fig. 2 of the supplementary material at the PBE/6-31G* level of theory and confirm that the two minima suggested by Horbury *et al.* previously are the only local minima with respect to the O–H dihedral bond angle.

Further to this, each of the minimum energy geometries underwent further optimization and frequency prediction with an implicit solvent model at the PBE0/cc-pVTZ level of theory; this result is shown in Fig. 3 of the supplementary material. Owing to the evident inaccuracy of this calculation, both in regard to absolute energy and energy differences between bands, it was determined that explicit solvent effects needed to be accounted for to construct an accurate model. Results for these more accurate models can be seen in Fig. 3 and in Fig. 4 in the supplementary material and are discussed *infra*.

Candidate structures for catechol in the *open* and *closed* conformers were optimized with two explicit acetonitrile molecules added. These structures are shown in Fig. 5 of the supplementary material. The lowest energy structure resulting from each of these candidates was further refined with geometry optimization and frequency prediction at the PBE0/cc-pVTZ level of theory. Common practice in comparing calculated vibrational frequencies to experiment involves rescaling all computational frequencies by a factor

close to 1 so that a calculated reference peak exactly matches the corresponding experimental result (an approach also applied for this system previously[26]). Scaling factors were determined for the *open* and *closed* conformers to be 0.966 and 0.975, respectively, for the PBE0/cc-pVTZ level of theory.

To verify that the optimized structures obtained are representative of realistic hydrogen-bonding interactions in this pairing of solvent and solute, we also generate several models containing explicit-solvent shells for the two structures. We apply a similar method to that previously used for explicit-solvent calculations for optical absorption spectra.[38,39] First, a classical molecular dynamics calculation is performed using the AMBER package.[40] For a given structure, the solute model was immersed in a 20 Å cube of explicit acetonitrile. For the *open* form, a dihedral angle restraint was applied to both C–C–O–H dihedral angles to ensure that the model could not flip between the *open* and *closed* conformers. The system was heated over 20 ps in the NVT ensemble wherein the temperature is raised from 0 to 300 K using the Langevin thermostat with a collision frequency of 2 ps^{-1}. This collision frequency is used for all further calculations. Following this, a 400 ps pressure equilibration is utilized in the PVT ensemble with the pressure fixed at 1 atm. Next, the system was equilibrated at a constant temperature of 300 K for 100 ps. Finally, snapshot generation proceeds via a further NVT ensemble run, this time with a fixed temperature of 300 K for 800 ps. 200 snapshots are taken by saving a configuration every 4 ps, with the intention being that the resulting snapshots are statistically uncorrelated in terms of the immediate solvent-solute environment. Three of these snapshots for each of the two systems were used for the following vibrational frequency calculations, with the full periodic box cut down to a cluster wherein any solvent molecule further away than 3 Å from the solute was removed. This results in models of size 56–74 atoms.

For each of these clusters, further geometry optimization and frequency calculations were performed, this time with the PBE/cc-pVDZ level of theory. This lower level of theory was used due to the increased computational effort associated with the larger models. A scaling factor was added to both the results for the *open* and *closed* form, 1.058 and 1.062, respectively; these results are shown in Fig. 4 of the supplementary material. For reference, the scaling factors associated with the models used above containing just two solvent molecules, were, at the same PBE/cc-pVDZ level of theory, 1.039 and 1.056 for the *open* and *closed* species, respectively, indicating a degree of consistency between the vibrational frequencies of the small and large models. It is worth noting that the calculations conducted with the PBE functional appear to underestimate the energy of the vibrational modes, whereas those conducted with the PBE0 functional appear to overestimate energy of the vibrational modes, in line with previous findings.[41]

III. RESULTS AND DISCUSSION

A. Examining the structure of monomeric catechol through theoretical frequency prediction

In previous work from our group, it was proposed that 4-TBC existed in two conformers in different solvent environments.[17] In nonpolar environments and the gas-phase, 4-TBC contains an intramolecular hydrogen bond. This structure is referred to, herein, as the *closed* conformer (Fig. 2). In polar solvents, the intramolecular hydrogen bond is broken, with the resulting structure referred to as an *open* conformer (Fig. 2). We investigated this dichotomy through a comparison of predicted vibrational frequencies in explicitly modeled solvent with experimental FTIR data; see Fig. 3.

In the O–H stretch region (3250–3600 cm^{-1}) of the experimental FTIR data of catechol in acetonitrile (5 mM), there are two bands with significant splitting, around 128 cm^{-1}. We attribute this splitting to the inhomogeneity between intramolecularly hydrogen bonded environments and the intermolecularly hydrogen bonded environments. As the *open* conformer does not have an intramolecular hydrogen bond, it is likely that the structure observed in acetonitrile is the *closed* conformer. This is further confirmed using of explicit-solvent frequency prediction with DFT. When predicting frequencies of the closed conformer, after applying the scaling factors discussed in Sec. II B, the results match the experimental data well. There are two bands predicted in the region of interest (red vertical lines) with an average splitting of 120 cm^{-1}, similar to the splitting observed experimentally (*cf.* 128 cm^{-1}). In this, the lower energy vibrational mode is associated with the intermolecularly bonded O–H stretch and the (weaker) higher energy vibrational mode is associated with the intramolecularly bonded O–H stretch; Table 1 in the supplementary material depicts these vibrational modes. This is in contrast to the predicted frequencies of the *open* form, which do not match the experimental result nearly as well. There are still two bands predicted in the region of interest although they are of a very similar energy with an average splitting of 7 cm^{-1} (blue vertical lines), with the predicted relative intensity of the secondary band being significantly weaker. The larger intensity band is associated with the asymmetric stretch of the O–H bonds with the weaker band being associated with the symmetric stretch; as before, Table 1 in the supplementary material depicts these vibrational modes. Given this, we re-evaluate previous findings and

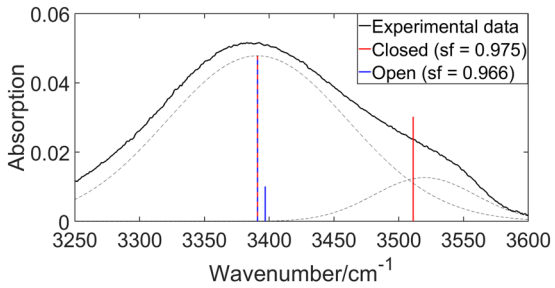

FIG. 3. A comparison between the experimental FTIR spectrum of catechol at 5 mM in acetonitrile (solid black line) and theoretical predictions of vibrational frequencies of catechol complexed with explicit acetonitrile solvent (vertical lines). The red lines are the predicted frequencies of the closed conformer, and the blue lines are the predicted frequencies of the open conformer. Where the red and blue lines lie on top of one another, the line is dashed red and blue. The experimental FTIR spectrum has been deconvolved into two Gaussian functions (shown through dashed black lines) after correcting for a small broad band associated with water absorption. This deconvolution serves to show the similarities between theoretical and experimental results. Calculated lines were shifted to align with the lower energy excitation (see text for details). Note: sf denotes scaling factor.

propose that the *closed* conformer of catechol (and 4-TBC) is the more likely candidate in acetonitrile.

When considering the effect of explicit solvent, it is important to use sufficient solvent molecules to accurately describe nonelectrostatic effects. Unfortunately, DFT is problematically expensive for hybrid functionals such as PBE0 with a large number of atoms. Because of this, more expensive calculations (PBE0/cc-pVTZ) were conducted on a system with just two solvent molecules. Calculations with a full shell of solvent molecules (3 Å radii) were conducted using a less expensive level of theory (PBE/cc-PVDZ) on three snapshots generated with molecular dynamics simulations. Further details can be found in Sec. II B and the supplementary material. As can be seen in Fig. 4 of the supplementary material, when using a full solvent shell, similar results are obtained to the more expensive calculations. In this case, this returns scaling factors of 1.062 and 1.058 for the *closed* and *open* conformers, respectively. This set of calculations predicted a splitting of 125 cm^{-1}. A caveat is warranted here: This result was obtained with only three snapshots and hence the variance in the calculated splittings was quite large, ≈35 cm^{-1}. This variation based on local environment is to be expected, however, and is reflected in the broadness of the corresponding experimental band. Vibrational O–H stretching bands are often broadened due to an array of local minima possible within different solvent configurations. Additionally, homogeneous broadening will also be influencing the peak widths. In order to properly sample the full array of potential configurations, one would need to run significantly more snapshots, at great computational cost. For our purposes, however, three snapshots seem to be sufficient to confirm that the methodology described previously using two solvent molecules gives a result in qualitative agreement to that with the full 3 Å solvent shell.

In recent work, Grieco *et al.* recorded a similar frequency spectrum when studying 3,5-di-*t*-butylcatechol and 3,5-di-*t*-butyl-*o*-quinone aggregates in cyclohexane.[42] They observed one broader band which they attributed to the intermolecularly hydrogen bonded O–H (referred to as bond "D") and one sharp band which they attributed to the intramolecularly hydrogen bonded O–H (referred to as bond "*b*"). The band we attribute to "D" (in the present work) was observed in acetonitrile at a similar frequency to that observed by Grieco *et al.*, albeit slightly shifted (at 3391 cm^{-1} as opposed to ≈3450 cm^{-1} observed previously), this is likely due to electrostatic effects. The band we attribute to "*b*" is broadened in acetonitrile (*cf.* sharp in cyclohexane); we plausibly suggest that this is due to a bifurcated hydrogen bond, similar to that shown in Fig. 6 in the supplementary material, which does not occur in cyclohexane.

We note that based on these results, it is unlikely that both the *open* and *closed* conformers are present. The splitting between the bands of the *open* form would not be visible even if it was present, given that they are only 7 cm^{-1} apart and have an intensity ratio of 1:15. However, we propose that there would be a significant difference in frequencies associated with the respective intermolecularly bonded O–H stretches of the *open* and *closed* forms. This is confirmed by the calculations, where the predicted energies for the lower energy band in *open* and *closed* conformers are 32 cm^{-1} apart. As we only see one primary band in the experimental spectrum, the *open* conformer is likely not present in a measurable quantity. This difference is not seen in Fig. 3 as both peaks were heterogeneously scaled and therefore are on top of one another. This difference can, however, be seen in Table 1 in the supplementary material.

Finally, Varfolomeev *et al.* noted that the presence of a basic species hydrogen bonded to catechol could weaken the internal hydrogen bond.[25] In our calculated geometries, when moving from catechol in implicit solvent to catechol with two explicit solvent molecules present, we observe an increase in bond-length from 2.10 Å to 2.25 Å. While 2.25 Å is still well within the expected bond length for hydrogen bonding, it is clear that the internal hydrogen bond is being weakened by the presence of the solvent. We do not measure the strength of the hydrogen bonding and to what degree it is weakened by collaborative effects from the basic acetonitrile as it is beyond the scope of this work, although it would definitely be an interesting avenue for future research.

We close this section noting that it has been suggested in the literature that guaiacol (2-methoxyphenol) exhibits the same *open* and *closed* behavior in solution as was previously suggested for catechol.[22] As guaiacol has no intermolecular hydrogen bond in the *closed* form, it is unlikely it behaves analogously with catechol. The lack of this intermolecular hydrogen bond will prevent aggregation and solvent-solute hydrogen bonding interactions. Furthermore, the *open* form of guaiacol is also likely to behave differently to that of catechol. As there is no internal hydrogen bond, the collaborative effects discussed by Varfolomeev *et al.* will not be present.[25] We therefore make no suggestion about the structure of guaiacol in polar solution based on the present work.

B. Transient electronic absorption spectroscopy results

The previous measurements by Horbury *et al.* in 4-TBC showed that the lifetime of the S_1 state in cyclohexane is significantly shorter than that in acetonitrile. Following our discussion *supra* regarding the absence of the previously predicted *open* conformer, we sought an alternative explanation for this difference in lifetime. For this, TEAS was conducted on catechol in acetonitrile at two different concentrations: 5 mM and 75 mM. Figure 4 shows representative TAS at 5 mM (top) and 75 mM (bottom) at four different pump-probe time-delays (Δt).

Two major points are worth acknowledging at this stage. First, the absorption feature at 390 nm associated with the formation of the catechoxyl radical is present in both cases; however, it is clearly much weaker compared to previous work in cyclohexane.[17–19] The size of this radical feature at 75 mM is consistent with previous observations in acetonitrile in a 35 mM solution. In 5 mM solution, however, it appears to be even further depleted, the reason for this will be discussed shortly. Second, it can clearly be seen that catechol in 5 mM solution decays (from the S_1 state) much faster than in 75 mM solution. Owing to this, a feature which resembles a triplet state can be more clearly evidenced at Δt = 2000 ps.[17,20] This feature has a maximum at below 350 nm and appears to slope across the entire spectral window of the probe. Interestingly, this agrees with Gauden *et al.* who find this same triplet state formation in their studies of dihydroxyindole (Fig. 1), further verifying the validity of this bottom-up approach.[17,43]

The decay of the excited state for each of these concentrations was studied in more detail by examining transient slices across the full set of time delays. These transients were obtained by integrating

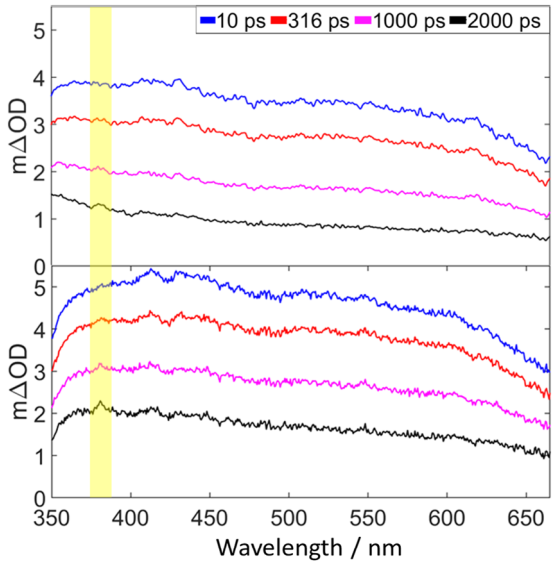

FIG. 4. Selected TAS at different Δt values of catechol in acetonitrile at (top) 5 mM and (bottom) 75 mM, following photoexcitation at 267 nm. The yellow bar serves to highlight the absorption of the catechoxyl radical species.

a 5 nm slice centered on the probe wavelength of 450 nm; these are shown in Fig. 5. This wavelength was selected as the radical photoproduct does not absorb in this region, an approach also followed by Horbury *et al.*[17] To extract the dynamical information, these transients were fit with a biexponential decay function which was convolved with a Gaussian function to model our instrument response function (≈80 fs). From these transients, two time-constants were extracted, τ_1 and τ_2.

The time-constant τ_1 was 70 ± 40 fs and 450 ± 50 fs for 5 mM and 75 mM concentration solutions, respectively. When studying 4-TBC in acetonitrile (35 mM), Horbury *et al.* observed similar time scales or τ_1 of 230 ± 20 fs, which they assigned to vibrational energy transfer as well as solvent rearrangement.[17,44] Based on this, we attribute the present τ_1 to a similar relaxation pathway.

Somewhat more interesting is the time-constant τ_2 extracted from the fit. The dynamics captured by this time-constant are

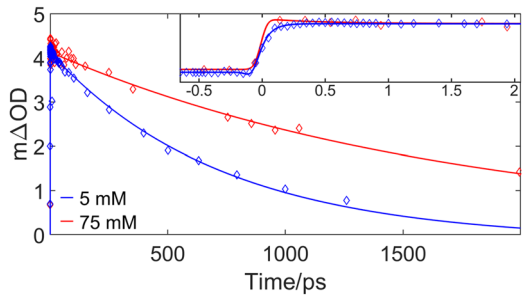

FIG. 5. TAS transients of catechol at a probe wavelength of 450 nm in acetonitrile at (blue) 5 mM and (red) 75 mM, following photoexcitation at 267 nm. Early time delays are shown in the inset.

TABLE I. Excited state lifetimes of catechol and 4-TBC in different solvents, cyclohexane (CHX) and acetonitrile (CH_3CN) at different concentrations. α and β denote, respectively, data taken from Horbury *et al.*[17] and Grieco *et al.*[26] in 4-TBC. Remaining data correspond to the present work on catechol.

Concentration (mM)	Lifetime in CH_3CN (ps)	Lifetime in CHX (ps)
5	730 ± 30	$12.15 \pm 0.3^{\beta}$
35	$1700 \pm 100^{\alpha}$	$18 \pm 1^{\alpha}$
75	1700 ± 200	$154 \pm 2^{\beta}$

assigned to depletion of the excited S_1 state. This will depend on the potential for O–H dissociation and access to the S_0/S_1 IC pathway. The lifetime observed for the S_1 state of catechol in acetonitrile at 5 mM was 0.73 ± 0.03 ns, increasing to 1.7 ± 0.2 ns for 75 mM. Table I collates the time-constants from the present work on catechol and that of Horbury *et al.* and Grieco *et al.* on 4-TBC, in cyclohexane and acetonitrile at different solvent concentrations.[17,26] The relative amplitudes of these exponential functions are displayed in Table 2 of the supplementary material.

When studying catechol in acetonitrile at 35 mM, Horbury *et al.* observed an S_1 lifetime of 1.7 ns. We observe this same lifetime at 75 mM concentration. This suggests that Horbury *et al.* were likely observing the properties of aggregated 4-TBC in their previous work;[17] we add here that Grieco *et al.* noted that 38 mM 4-TBC in cyclohexane is ≈50% aggregated. It was proposed that this accounts for shorter lifetime of τ_2 measured at 5 mM vs what Horbury *et al.* measured at 35 mM.[26]

Figure 6 shows a schematic of the different decay pathways available to the S_1 state of catechol. As stated in previous work, the primary route of S_1 decay for monomeric 4-TBC in cyclohexane, and likely catechol, is through homolytic fission of the nonintramolecularly bound O–H bond and the formation of the catechoxyl radical.[17,26] This is identified through the growth of an absorption feature at 390 nm.[18,19] In this case, the energy barrier along the reaction

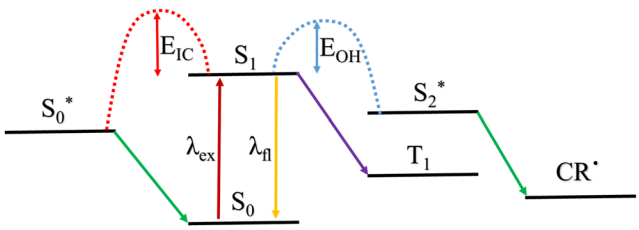

FIG. 6. A schematic to show different decay pathways for the S_1 state of catechol. The maroon arrow labeled λ_{ex} denotes the pump pulse, which excites the system into the S_1 state; this is, in this case, at 267 nm. This S_1 state can undergo either IC through transition to a vibrationally hot S_0 state (denoted S_0^*) or O–H dissociation transition to yield the catechoxyl radical (CR•), mediated through transition to the S_2 state ($^1\pi\sigma^*$). Both of these are barriered processes, both of which have suggested barriers (labeled E_{IC} and E_{OH}) which govern the excited state behavior of catechol. If barriers are sufficiently large, then two further paths become available: fluorescence and intersystem crossing; these are represented by the yellow (labeled λ_{fl}) and purple arrows, respectively.

coordinate associated with O–H dissociation, which we call E_{OH}, is small. This O–H dissociation pathway has previously been attributed to tunneling from the S_1 $^1\pi\pi^*$ state to the dissociative (along O–H) $^1\pi\sigma^*$ state (S_2).[45] Owing to the small energy barrier along this pathway (denoted E_{OH} in Fig. 6), the process is therefore ultrafast (≈12 ps), outcompeting other processes.

It has been shown previously that when aggregated in cyclohexane, the S_1 state of 4-TBC decayed through two competing mechanisms: (1) O–H dissociation (*vide supra*) and (2) IC mediated via an S_1/S_0 conical intersection.[26] This was seen through the apparent reduction in the signal intensity of the catechoxyl radical feature although this was somewhat challenging to observe due to a solvatochromic shift and broadening caused by hydrogen bonding. These studies revealed a lifetime for IC of 154 ps, meaning that O–H dissociation has sufficiently been hindered to enable this pathway to be competitive (with O–H dissociation). An increase in E_{OH} from 0.1 eV for free O–H dissociation to 0.51 eV for O–H dissociation when bonded via intermolecular hydrogen bond has been calculated previously.[26] This increased barrier height resulted in a lifetime for O–H dissociation of 190 ps. This was broadly in agreement with the previous literature in which the effect of intermolecular hydrogen bonding was observed in phenol clusters in the gas-phase.[46] It was shown that hydrogen bonding causes the dissociative S_2 ($^1\pi\sigma^*$) state to become bound at higher bond distances. This work was based on calculations previously conducted on dimeric water.[26,47]

Returning to present studies, when studying catechol in acetonitrile at 5 mM, a concentration that we consider catechol to be primarily monomeric, we observe a τ_2 of 730 ps. This lifetime is significantly longer than the lifetime of both IC and O–H dissociation seen in 4-TBC at 5 mM in cyclohexane (see above). There are multiple factors that could be influencing the increase in τ_2. The first of which are the barriers along the reaction coordinates toward IC and O–H bond dissociation (E_{IC} and E_{OH}, respectively), which must be increasing in order for a lifetime of 730 ps to be observed. This could be a consequence of energy level stabilization or destabilization by the solvent/aggregate. To garner a quantitative picture, one would need to theoretically determine the relative energy landscapes associated with each of these processes as well as conduct target analysis of the TAS data. The latter was previously conducted by Grieco *et al.* when studying these processes in 4-TBC when aggregated in cyclohexane.[26] This goes beyond the scope of the present study. Ultimately, the slowing of these two processes has allowed two other mechanisms to begin to compete. The first is an intersystem crossing pathway, which is evidenced in Fig. 4 by the growth of an absorption feature in the TAS around 350 nm which slopes across our entire spectral window of our probe.[20] This triplet state was also observed by Horbury *et al.*; however, as discussed previously, it is likely that they were observing an aggregated species. The second process is fluorescence, which is also likely occurring, as discussed in Sec. I. As can be seen in Fig. 4, the signal associated with the catechoxyl radical absorption is almost not visible in this case owing to the degree of competition from intersystem crossing, and fluorescence (in addition to IC).

When observing aggregated catechol in acetonitrile, at 75 mM, τ_2 increases further to 1.7 ns. This is the same lifetime that was previously observed by Horbury *et al.* in 35 mM 4-TBC in acetonitrile.[17] This is over double that of the monomeric species in acetonitrile. We speculate that E_{IC} is increasing, viewed through the aggregate taking up a rigid structure which hinders the geometric rearrangement necessary to approach the conical intersection geometry along the IC reaction pathway. Naturally, this may also likely lead to an increase in catechoxyl radical formation (which could explain the increased radical signature seen in Fig. 4), fluorescence, and intersystem crossing although we are unable to directly measure these quantum yields from the present experimental setup.

IV. CONCLUSIONS

In this paper, we have considered solvent effects on the lifetime of the S_1 state of catechol in solution drawing on (primarily) two previous studies, as well as our present findings. Horbury *et al.* previously suggested that 4-TBC, a catechol mimic, existed in an *open* conformer when in polar solvents and a *closed* conformer when in nonpolar solvents or the gas-phase.[17] We argue this is not the case by showing that in acetonitrile, a polar solvent, catechol is in the *closed* form. This was shown through a comparison of predicted vibrational frequencies in explicitly modeled solvent allied with experimental FTIR data. In the O–H stretch region (3200–3600 cm^{-1}) of the experimental FTIR spectrum of catechol in acetonitrile (5 mM), there are two peaks with significant splitting, around 128 cm^{-1}. This was compared to frequency prediction with DFT using an explicit solvent model. When considering the *closed* conformer, there were two peaks predicted in the region of interest with an average splitting of 120 cm^{-1}; this matches well with what was observed experimentally. The predicted frequencies of the *open* conformer still yield two peaks predicted in the region of interest. They are, however, of a very similar energy with an average splitting of 7 cm^{-1}; we suggest the *closed* conformer is the species present in acetonitrile. While it has been shown by Huijser *et al.* that O–H dissociation in the catechol moiety is not the primary decay pathway when considering DHICA, it is still valuable when considering a bottom-up approach to know the exact geometry of catechol in different solvents.[48] The existence of the *closed* form in DHICA in polar solvents will change the way we view the structure of this important eumelanin building block.

Given that the *open* vs *closed* dichotomy is not the cause of the observed differences in the S_1 lifetime of catechol in cyclohexane and acetonitrile, we aimed to find other explanations. Grieco *et al.* suggested that when aggregated, 4-TBC undergoes intermolecular hydrogen bonding, the barrier along the O–H dissociation (E_{OH}) coordinate is significantly increased.[26] This leads to an increase in the time taken to undergo O–H dissociation (from 12 ps up to 190 ps) which allows IC to the ground state to occur as a competing mechanism. In acetonitrile at 5 mM, which we assume catechol to be primarily monomeric, the lifetime observed for S_1 of catechol was 713 ps. From this, it is reasonable to suggest that both the IC path and the O–H dissociation are retarded significantly by the change in the solvent. When studying aggregated catechol (75 mM), the lifetime of the S_1 state increases further still to around 1700 ps. We suggest that aggregation disfavors IC, possibly due to a rigid structure decreasing the molecules ability to reach a geometric conical intersection. This work has shown that explicit-solvent methodology is key when calculating the vibrational frequencies of molecules in interacting solvent. Combining this with highly complementary steady-state and transient absorption spectroscopy enables us to gain

key dynamical insights into how a prominent eumelanin building block behaves when in polar, hydrogen bond accepting solvents both as a monomer and as an aggregated species.

While this work was under review, Grieco *et al.* published a further related work (Ref. 49), which addresses the effect of inter- and intramolecular hydrogen bonding on the ultrafast photochemistry of catechol. This was achieved through varying concentrations of Et_2O, resulting in three different hydrogen bonding arrangements.

SUPPLEMENTARY MATERIAL

The supplementary material for this paper includes a fitted time-zero artifact for the TEAS setup in acetonitrile solvent; a two-dimensional plot of S_0 energy of catechol with respect to the dihedral angles of the two OH groups; calculated frequencies for catechol in the *open* and *closed* conformer as calculated using both an implicit solvent model and an explicit solvent shell; the starting geometries for the two-solvent frequency calculations; the vibrational modes in the O–H stretch region associated with the two-solvent frequency calculations; and a representation of the three different types of hydrogen bonding possible in the *closed* conformer of catechol in acetonitrile; and a table of amplitudes for the fitted biexponential functions described in Sec. III B.

The underlying data of this publication can be accessed via the Zenodo Archive at DOI: 10.5281/zenodo.3241438.

ACKNOWLEDGMENTS

M.A.P.T. thanks the EPSRC for a doctoral studentship through the EPSRC Centre for Doctoral Training in Molecular Analytical Science, Grant No. EP/L015307/1. M.D.H. thanks the Leverhulme Trust for postdoctoral funding. Computing facilities were provided by the Scientific Computing Research Technology Platform of the University of Warwick. We acknowledge the use of Athena at HPC Midlands+, which was funded by the EPSRC by Grant NO. EP/P020232/1, in this research, as part of the HPC Midlands+ consortium. N.D.M.H. acknowledges the support of EPSRC Grant No. EP/P02209X/1 and Royal Society Research Grant No. RG150013. V.G.S. is grateful to the EPSRC for an equipment grant (No. EP/N010825) and the Royal Society and the Leverhulme Trust for a Royal Society Leverhulme Trust Senior Research Fellowship.

REFERENCES

[1]J. Moan, "Visible light and UV radiation," in *Radiation at Home, Outdoors and in the Workplace* (Scandinavian Publisher, Oslo, 2001), pp. 69–85.
[2]N. Agar and A. R. Young, "Melanogenesis: A photoprotective response to dna damage?," Mutat. Res., Fundam. Mol. Mech. Mutagen. **571**, 121–132 (2005).
[3]N. Kollias, R. M. Sayre, L. Zeise, and M. R. Chedekel, "New trends in photobiology: Photoprotection by melanin," J. Photochem. Photobiol., B **9**, 135–160 (1991).
[4]M. A. Weinstock, "Epidemiology of melanoma," *Current Research and Clinical Management of Melanoma* (Springer, 1993), pp. 29–56.
[5]H. Z. Hill, "The function of melanin or six blind people examine an elephant," Bioessays **14**, 49–56 (1992).
[6]A. Büngeler, B. Hämisch, and O. Strube, "The supramolecular buildup of eumelanin: Structures, mechanisms, controllability," Int. J. Mol. Sci. **18**, 1901 (2017).
[7]S. Ito, "Reexamination of the structure of eumelanin," Biochim. Biophys. Acta, Gen. Subj. **883**, 155–161 (1986).
[8]W. L. Cheun, "The chemical structure of melanin," Pigm. Cell Res. **17**, 422–423 (2004).
[9]J. Simon and S. Ito, "The chemical structure of melanin-reply," Pigm. Cell Res. **17**, 423–424 (2004).
[10]E. Kaxiras, A. Tsolakidis, G. Zonios, and S. Meng, "Structural model of eumelanin," Phys. Rev. Lett. **97**, 218102 (2006).
[11]W. L. Morison, "What is the function of melanin?," Arch. Dermatol. **121**, 1160–1163 (1985).
[12]P. U. Giacomoni, "Open questions in photobiology III. Melanin and photoprotection," J. Photochem. Photobiol., B **29**, 87–89 (1995).
[13]H. Z. Hill and G. J. Hill, "Uva, pheomelanin and the carcinogenesis of melanoma," Pigm. Cell Res. **13**, 140–144 (2000).
[14]L. Panzella, G. Gentile, G. D'Errico, N. F. Della Vecchia, M. E. Errico, A. Napolitano, C. Carfagna, and M. d'Ischia, "Atypical structural and π-electron features of a melanin polymer that lead to superior free-radical-scavenging properties," Angew. Chem., Int. Ed. **52**, 12684–12687 (2013).
[15]C. Frontana and I. González, "The role of intramolecular hydrogen bonding in the electrochemical behavior of hydroxy-quinones and in semiquinone stability," J. Braz. Chem. Soc. **16**(3A), 299–307 (2005).
[16]P. Meredith and T. Sarna, "The physical and chemical properties of eumelanin," Pigm. Cell Res. **19**, 572–594 (2006).
[17]M. D. Horbury, L. A. Baker, W.-D. Quan, J. D. Young, M. Staniforth, S. E. Greenough, and V. G. Stavros, "Bridging the gap between the gas phase and solution phase: Solvent specific photochemistry in 4-tert-butylcatechol," J. Phys. Chem. A **119**, 11989–11996 (2015).
[18]E. Land and G. Porter, "Primary photochemical processes in aromatic molecules. Part 7.—Spectra and kinetics of some phenoxyl derivatives," Trans. Faraday Soc. **59**, 2016–2026 (1963).
[19]O. Brede, S. Kapoor, T. Mukherjee, R. Hermann, and S. Naumov, "Diphenol radical cations and semiquinone radicals as direct products of the free electron transfer from catechol, resorcinol and hydroquinone to parent solvent radical cations," Phys. Chem. Chem. Phys. **4**, 5096–5104 (2002).
[20]D. Bent and E. Hayon, "Excited state chemistry of aromatic amino acids and related peptides. I. Tyrosine," J. Am. Chem. Soc. **97**, 2599–2606 (1975).
[21]Y. Zhang, T. A. Oliver, M. N. Ashfold, and S. E. Bradforth, "Contrasting the excited state reaction pathways of phenol and para-methylthiophenol in the gas and liquid phases," Faraday Discuss. **157**, 141–163 (2012).
[22]S. E. Greenough, M. D. Horbury, J. O. Thompson, G. M. Roberts, T. N. Karsili, B. Marchetti, D. Townsend, and V. G. Stavros, "Solvent induced conformer specific photochemistry of guaiacol," Phys. Chem. Chem. Phys. **16**, 16187–16195 (2014).
[23]A. Douhal, F. Lahmani, and A. H. Zewail, "Proton-transfer reaction dynamics," Chem. Phys. **207**, 477–498 (1996).
[24]J. L. Navarrete and F. Ramírez, "A study by Raman spectroscopy and the semiempirical am1 method on several 1, 2-dihydroxybenzene solutions," Spectrochim. Acta, Part A **49**, 1759–1767 (1993).
[25]M. A. Varfolomeev, D. I. Abaidullina, A. Z. Gainutdinova, and B. N. Solomonov, "FTIR study of h-bonds cooperativity in complexes of 1, 2-dihydroxybenzene with proton acceptors in aprotic solvents: Influence of the intramolecular hydrogen bond," Spectrochim. Acta, Part A **77**, 965–972 (2010).
[26]C. Grieco, F. R. Kohl, Y. Zhang, S. Natarajan, L. Blancafort, and B. Kohler, "Intermolecular hydrogen bonding modulates O-H photodissociation in molecular aggregates of a catechol derivative," Photochem. Photobiol. **95**, 163 (2018).
[27]J. Dearden, "Investigation of the self-association of phenols and anilines by ultraviolet spectroscopy," Can. J. Chem. **41**, 2683–2691 (1963).
[28]K. B. Whetsel and J. Lady, "Self-association of phenol in nonpolar solvents," in *Spectrometry of Fuels* (Springer, 1970), pp. 259–279.
[29]D. Gerrard and W. Maddams, "Solvent effects in uv absorption spectra. I. Phenol in cyclohexane ethanol mixtures," Spectrochim. Acta, Part A **34**, 1205–1211 (1978).
[30]S. E. Greenough, G. M. Roberts, N. A. Smith, M. D. Horbury, R. G. McKinlay, J. M. Żurek, M. J. Paterson, P. J. Sadler, and V. G. Stavros, "Ultrafast photoinduced ligand solvolysis of *cis*-[Ru (bipyridine)$_2$ (nicotinamide)$_2$]$^{2+}$: Experimental and theoretical insight into its photoactivation mechanism," Phys. Chem. Chem. Phys. **16**, 19141–19155 (2014).

[31]M. Horbury, W.-D. Quan, A. Flourat, F. Allais, and V. Stavros, "Elucidating nuclear motions in a plant sunscreen during photoisomerization through solvent viscosity effects," Phys. Chem. Chem. Phys. **19**, 21127–21131 (2017).
[32]M. Valiev, E. J. Bylaska, N. Govind, K. Kowalski, T. P. Straatsma, H. J. Van Dam, D. Wang, J. Nieplocha, E. Apra, T. L. Windus *et al.*, "NWChem: A comprehensive and scalable open-source solution for large scale molecular simulations," Comput. Phys. Commun. **181**, 1477–1489 (2010).
[33]J. P. Perdew, K. Burke, and M. Ernzerhof, "Generalized gradient approximation made simple," Phys. Rev. Lett. **77**, 3865 (1996).
[34]E. R. Davidson, "Comment on 'comment on Dunning's correlation-consistent basis sets'," Chem. Phys. Lett. **260**, 514–518 (1996).
[35]A. Klamt and G. Schüürmann, "COSMO: A new approach to dielectric screening in solvents with explicit expressions for the screening energy and its gradient," J. Chem. Soc., Perkin Trans. 2 **1993**, 799–805.
[36]D. M. York and M. Karplus, "A smooth solvation potential based on the conductor-like screening model," J. Phys. Chem. A **103**, 11060–11079 (1999).
[37]P. Winget, D. M. Dolney, D. J. Giesen, C. J. Cramer, and D. G. Truhlar, *Minnesota Solvent Descriptor Database* (Deptartment of Chemistry and Supercomputer Institute, University of Minnesota, Minneapolis, MN, 1999).
[38]M. A. Turner, M. D. Horbury, V. G. Stavros, and N. D. Hine, "Determination of secondary species in solution through pump-selective transient absorption spectroscopy and explicit-solvent TDDFT," J. Phys. Chem. A **123**, 873 (2019).
[39]T. J. Zuehlsdorff, P. D. Haynes, M. C. Payne, and N. D. M. Hine, "Predicting solvatochromic shifts and colours of a solvated organic dye: The example of nile red," J. Chem. Phys. **146**, 124504 (2017).
[40]D. A. Case, J. T. Berryman, R. M. Betz, D. S. Cerutti, T. E. Cheatham III, T. A. Darden, R. E. Duke, T. J. Giese, H. Gohlke, A. W. Goetz, N. Homeyer, S. Izadi, P. Janowski, J. Kaus, A. Kovalenko, T. S. Lee, S. LeGrand, P. Li, T. Luchko, R. Luo, B. Madej, K. M. Merz, G. Monard, P. Needham, H. Nguyen, H. T. Nguyen, I. Omelyan, A. Onufriev, D. R. Roe, A. Roitberg, R. Salomon-Ferrer, C. L. Simmerling, W. Smith, J. Swails, R. C. Walker, J. Wang, R. M. Wolf, X. Wu, D. M. York, and P. A. Kollman, *Amber 2015*, University of California, San Francisco, 2015.
[41]I. Alecu, J. Zheng, Y. Zhao, and D. G. Truhlar, "Computational thermochemistry: Scale factor databases and scale factors for vibrational frequencies obtained from electronic model chemistries," J. Chem. Theory Comput. **6**, 2872–2887 (2010).
[42]C. Grieco, J. M. Empey, F. R. Kohl, and B. Kohler, "Probing eumelanin photoprotection using a catechol: Quinone heterodimer model system," Faraday Discuss. **216**, 520 (2019).
[43]M. Gauden, A. Pezzella, L. Panzella, A. Napolitano, M. d'Ischia, and V. Sundström, "Ultrafast excited state dynamics of 5, 6-dihydroxyindole, a key eumelanin building block: Nonradiative decay mechanism," J. Phys. Chem. B **113**, 12575–12580 (2009).
[44]E. W. Castner, Jr., M. Maroncelli, and G. R. Fleming, "Subpicosecond resolution studies of solvation dynamics in polar aprotic and alcohol solvents," J. Chem. Phys. **86**, 1090–1097 (1987).
[45]A. S. Chatterley, J. D. Young, D. Townsend, J. M. Żurek, M. J. Paterson, G. M. Roberts, and V. G. Stavros, "Manipulating dynamics with chemical structure: Probing vibrationally-enhanced tunnelling in photoexcited catechol," Phys. Chem. Chem. Phys. **15**, 6879–6892 (2013).
[46]V. Poterya, L. Šištík, P. Slavíček, and M. Fárník, "Hydrogen bond dynamics in the excited states: Photodissociation of phenol in clusters," Phys. Chem. Chem. Phys. **14**, 8936–8944 (2012).
[47]G. Quinkert, "Photochemistry of linearly conjugated cyclohexadienones in solution," Pure Appl. Chem. **33**, 285–316 (1973).
[48]A. Huijser, A. Pezzella, J. K. Hannestad, L. Panzella, A. Napolitano, M. d'Ischia, and V. Sundström, "UV-dissipation mechanisms in the eumelanin building block DHICA," ChemPhysChem **11**, 2424–2431 (2010).
[49]C. Grieco, A. T. Hanes, L. Blancafort, and B. Kohler, "Effects of intra-and intermolecular hydrogen bonding on O–H bond photodissociation pathways of a catechol derivative," J. Phys. Chem. A **123**, 5356–5366 (2019).